Geomechanics and Engineering, *Vol. 42, No. 6 (2025) 409-423*
https://doi.org/10.12989/gae.2025.42.6.409

Role of geogrid-encased deep soil mixing columns in enhancing foundation performance on the reinforced collapsible sandy Sabkha soil

Mohamed Elsawy*[1,2], Abderrahim Lakhouit[3], Turki S. Alahmari[4], Hossam AbdelMeguid[5,6] and Mahmoud Shaban[7,8]

[1]*Department of Civil Engineering, Faculty of Engineering, Geotechnical and Foundations Engineering at University of Tabuk, Tabuk 71491, Saudi Arabia*
[2]*Department of Civil Engineering, Faculty of Engineering, Geotechnical and Foundations Engineering at Aswan University, Aswan 81542, Egypt*
[3]*Department of Civil Engineering, Faculty of Engineering, Environmental Engineering at University of Tabuk, Tabuk 71491, Saudi Arabia*
[4]*Department of Civil Engineering, Faculty of Engineering, University of Tabuk, Tabuk 71491, Saudi Arabia*
[5]*Department of Mechanical Engineering, Faculty of Engineering, University of Tabuk, 47913 Tabuk, Saudi Arabia*
[6]*Department of Mechanical Power Engineering, Faculty of Engineering, Mansoura University, El-Mansoura 35516, Egypt*
[7]*Department of Electrical Engineering, College of Engineering, Qassim University, Saudi Arabia*
[8]*Department of Electrical Engineering, Faculty of Engineering, Aswan University, Aswan 81542, Egypt*

(*Received December 13, 2024, Revised August 22, 2025, Accepted September 3, 2025*)

Abstract. The current research aims to reinforce collapsible Sabkha soil by encased deep soil mixing columns (EDSMCs). Full-scale three-dimensional numerical models are created to analyze the performance of footings on both untreated and treated soil. Various parameters such as columns configuration, lime content, collapse index and geogrid stiffness are considered**.** The results demonstrated that the conventional DSMCs significantly increase the bearing capacity of the collapsible soil under immersion conditions, up to three times that of non-treated soil. However, the bearing capacity of the footing on the reinforced soil still requires further enhancement. Utilizing geogrid encasement for DSMCs improves effectively the foundation bearing capacity, and minimizes the foundation settlement and the columns lateral bulging compared to conventional DSMCs. The minimum settlement and lateral bulging, and the greater loads carried by EDSMCs are achieved when utilizing higher geogrid stiffness**.** In addition to the numerical analyses, multiple machine learning models including Logistic Regression (LR), Nonlinear Regression (NLR), Support Vector Machine (SVM), Gaussian Process Regression (GPR), Random Forest (RF), Decision Tree (DT), and Extreme Gradient Boosting (XGBoost) are developed. These models exhibited strong performance in predicting the properties of treated Sabkha soil, with Coefficient of Determination (R^2-Score) exceeding 0.95. The machine learning analyses support the findings of the numerical analyses, emphasizing the significant role of geogrid encasement in enhancing footing performance on the reinforced soil.

Keywords: collapsed settlement; deep soil mixing columns; geosynthetics; load transfer; machine learning

1. Introduction

Collapsible soils pose significant challenges for geotechnical engineers during construction projects. These soils can undergo significant volume reduction and loss of strength when subjected to changes in moisture content or/and increased loads (Feda 1988, Houston *et al.* 1988, Derbyshire 2001, Houston *et al.* 2001, Peng *et al.* 2006, Lommler and Bandini 2015). Collapsible soils are located in several countries around the world, including China, Russia, United States, Germany, Algeria, Egypt, and Saudi Arabia (Johnson *et al.* 1978, Phien-wej *et al.* 1992, Rogers *et al.* 1994, Rogers 1995, Al-Rawas 2000, Nouaouria *et al.*2008; Ryashchenko *et al.* 2008, Gaaver 2012). Sandy Sabkha soil is considered a main type of the collapsible soils. The presence of salts in sandy Sabkha soils plays a significant role in their collapsible behaviour. The salts act as a binder or cementing agent, holding the soil particles together and providing some degree of stability. However, when the soil is wetted, the salts dissolve, weakening the bonding between the particles and reducing the soil's strength and load-bearing capacity. (Clemence and Finbarr 1981, Stipho 1985, Ismael 1993, Al-Amoudi and Abduljauwad 1995, Al-Amoudi 2002). The collapsible behaviour of the sandy Sabkha soil was detected and studied by several research either coastal Sabkha soil (Abduljauwad 1997, Al-Amoudi *et al.* 1997, Sabtan 2005, Sakr *et al*. 2008) or inland Sabkha soil (Elsawy and Lakhouit 2021). Therefore, constructing structures on natural collapsible soils can indeed pose a significant risk. However, there are various treatment and improvement methods available to mitigate these risks and enhance the stability of the soil. One effective approach is the use of reinforcement techniques, such as geosynthetics or column elements.

Deep soil mixing columns (DSMCs) involve the mechanical mixing or injection of a stabilizing agent, such

*Corresponding author, Associate Professor
E-mail: melsawy@ut.edu.sa

ISSN: 2005-307X (Print), 2092-6219 (Online)

as cement or lime into the soil to create vertical columns. These columns increase the soil's shear strength, stiffness, and load-bearing capacity (Bouassida *et al*. 2020, Bouassida *et al.* 2022). Furthermore, DSMCs are designed to enhance fine soil permeability, allowing for better drainage, and reducing the risk of water logging (Chen *et al.* 2003, Chen *et al.* 2008, Nguyen *et al.* 2016, Liu *et al.* 2017, A Rashid *et al.* 2017, Bouassida *et al.* 2020, Alhamdi and Albusoda 2021, Liu *et al.* 2021). Recently, the Sabkha soil was reinforced by DSMCs using different binders and achieving effective improvement in settlement and bearing capacity (Jung *et al.* 2020, Hammad *et al.* 2023, Abas *et al.* 2024).

The binder material is responsible for binding the soil particles together and providing strength and stability to the treated soil (Makusa 2013, Pourakbar and Huat 2017). Most of past researchers utilized DSMCs binder of cement (Bouassida and Porbaha 2004, Esmaeili and Khajehei 2016, Liu *et al.* 2021, Oliaei *et al.* 2021, Abas *et al.* 2024) or other waste materials partially contributed instead of cement in the DSMCs binder (Jung *et al.* 2020, Alnunu *et al.* 2021, Disfani *et al.* 2021, Alnunu and Nalbantoglu 2022, Hammad *et al.* 2023, Pinheiro *et al.* 2024).

The use of hydrated lime as an alternative binder material in soil stabilization applications has gained attention due to its environmental benefits and superior engineering properties (Liu *et al.* 2020, Pourakbar and Huat 2017). Hydrated lime production results in notably lower carbon emissions compared to traditional cement manufacturing processes(Ebrahimi *et al.* 2023, Kang *et al.* 2019).

Studies such as those by Abbey and Ngambi (2015), Bouassida *et al.* (2022), and Larsson (2003) demonstrated the effectiveness and feasibility of hydrated lime as a binder DSMCs for soil stabilization purposes. Notably, Pakbaz and Farzi (2015) compared the performance of hydrated lime and cement in DSMCs, revealing that hydrated lime notably enhanced soil strength, decreased permeability, and bolstered the long-term stability of treated soil. From the structural point of view, conventional DSMCs sustain from excessive lateral bulging leading to their failure due to the weak lateral support from the saturated surrounding soil. Hence, encasement of DSMCs with geosynthetics materials solves the later problem and increases the overall bearing capacity (Ayadat *et al.* 2008, Elsawy 2013, Jaiswal and Kumar 2022). Recently, the concept of using geosynthetic-encased stone columns in collapsible soils was investigated by few researchers (Ayadat, and Hanna 2005, Araujo 2009, Al-Obaidy *et al.* 2015, Bahrami and Marandi 2021). But reinforcing collapsible soil with geogrid-encased DSMCs was not yet studied by past researchers.

Machine learning (ML) and artificial intelligence (AI) methodologies are versatile and can be effectively deployed across multiple facets of geotechnical engineering, such as data analytics, modeling, design enhancement, and risk evaluation (Dinarvand and Ardakani 2022, Pereira *et al.* 2023, Verma *et al.* 2023, Mahmoodi *et al.* 2024, Sert *et al.* 2024). Cutting-edge ML and AI models have been specifically crafted to forecast the ultimate bearing capacity of shallow foundations (Abiodun and Sangki 2023, Liu and Liang 2024). Furthermore, in parallel, these advanced technologies are instrumental in assessing and projecting soil enhancement through the utilization of geosynthetic materials (Raja and Shukla 2021, Raja *et al.* 2023). Based on the above, researchers have rarely explored the utilization of lime-based deep soil mixing columns to enhance collapsible sandy Sabkha soil in the previous studies. To the best of our knowledge until now, there is also no research investigated the improvement of collapsible sandy Sabkha soil with conventional or geogrid-encased deep soil mixing columns. Therefore, the current research focuses on enhancing collapsible sandy Sabkha soil using geogrid-encased deep soil mixing columns (EDSMCs). It aims to assess the performance of treated soil with EDSMCs under footing loads through full-scale 3D numerical models based on experimental studies. These models analyze load-settlement, load sharing, and lateral bulging curves, considering various parameters' impact on the reinforced soil behaviour. Additionally, the study explores ML techniques for designing and optimizing reinforced collapsible Sabkha soil. ML models, developed from numerical and experimental results, advance understanding of foundation performance on reinforced Sabkha soil with EDSMCs, marking a significant advancement in this underexplored field.

2. Material and methods

2.1 Material

The current study is related to the experimental study of Elsawy and Lakhouit (2021, 2023) containing basic and index properties of the sandy Sabkha soil. They conducted research on the sandy Sabkha soil from Tayma city in the Tabuk region of Saudi Arabia, focusing on its collapsible nature and stabilization using hydrated lime. The sandy Sabkha soil is classified as SP-SM according to USCS. Experimental tests were performed on untreated and lime-treated Sabkha soil samples under immersion conditions to assess the effectiveness of lime in mitigating collapsibility. Various tests such as modified compaction proctor, single oedometer, California Bearing Ratio (CBR), and direct shear tests were conducted to evaluate the properties of the soil and soil-lime mixtures. Hydrated lime was added at different percentages (5%, 10%, 15%, and 20%) to reduce the collapsible behaviour of the sandy Sabkha soil.

2.2 Numerical model

The study focuses on analyzing the impact of geogrid-encased DSMCs on the behaviour of collapsible Sabkha soil under square foundation loads. A 3D model was developed using the Plaxis 3D program, considering detailed geometric and material properties for the foundation, soil layers, and EDSMCs. The reinforced concrete square foundation had specific dimensions (3.0 m on each side) and thickness (0.70 m), placed at a level of 1.5 m on an 8.5 m thick layer of sandy Sabkha soil, with a layer of sand fill above it. The model included various configurations of EDSMCs with a depth of 8.5 m, differing in lime

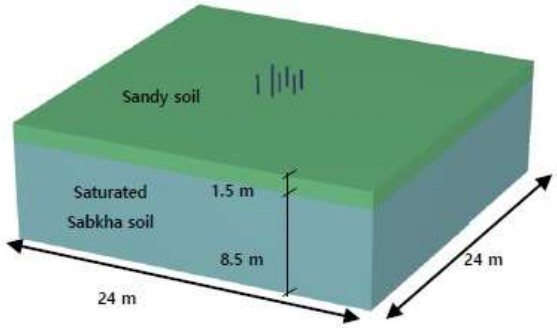

(a)

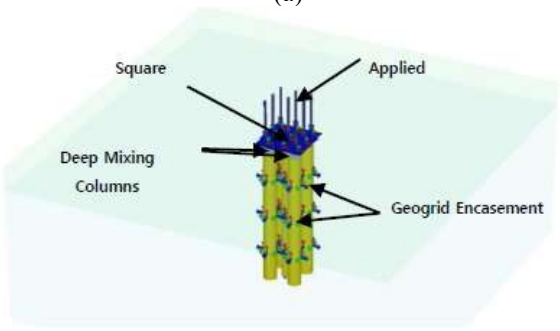

(b)

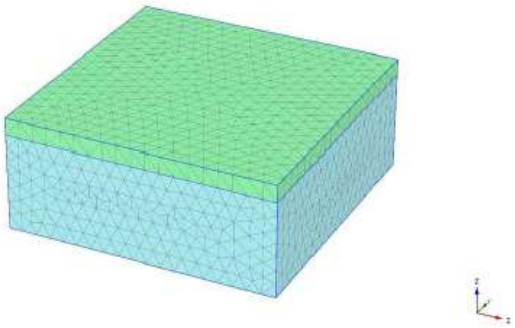

(c)

Fig. 1 3D Modeling, (a) Full model parts, (b) Applied loads on foundations, DSMCs and geogrid encasement and (c) FEM mesh

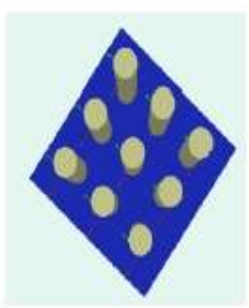

(a) d = 0.4 m and s/d = 2, (Ar = 0.13)

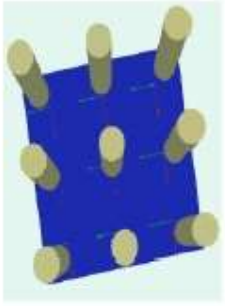

(b) d = 0.4 m and s/d = 3, (Ar = 0.13)

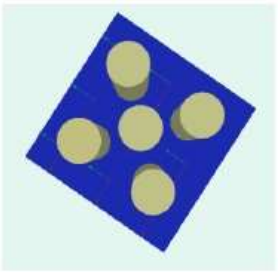

(c) d = 0.6 m and s/d = 2, (Ar = 0.16)

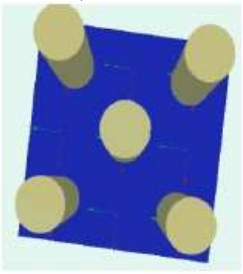

(d) d = 0.6 m and s/d = 3, (Ar = 0.16)

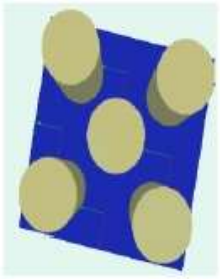

(e) d = 0.8 m and s/d = 2, (Ar = 0.28)

Fig. 2 DSMCs orientations under the square foundations

percentages, column geometries (diameters and spacing distances), and area replacement ratios. EDSMCs, made of saturated Sabkha soil mixed with lime, had diameters of 0.4 m, 0.6 m, and 0.8 m, with spacing ratios of 2 and 3. The top of DSMCs was positioned below the sand replacement layer, considering a groundwater table 1.0 m below the ground surface, as depicted in Figs. 1(a) and 1(b). Boundary conditions restricted perpendicular displacements, assuming a hard rock layer at the base. A fine mesh was utilized in the model, comprised of tetrahedral elements for soils and triangular plate elements for the footing, as illustrated in Fig. 1(c). The saturated sandy Sabkha soil and DSMCs were modeled using the Mohr-Coulomb failure criterion under drained conditions. The reinforced concrete square footing was represented as a linear-elastic plate.

The DSMCs were reinforced with geogrid encasement modeled as a linear elastic continuum element without bending stiffness, using elastic flexible elements transmitting only axial tension forces. Different geogrid stiffness values (800 kN/m, 2000 kN/m, 5000 kN/m, and 10,000 kN/m) were employed in the model. The geogrid encasement was simulated as a Geogrid element with specific axial stiffness values. Input parameters for the soils, DSMCs, and footing were obtained from experimental studies, presented in Tables 1 and 2. Once initial stresses were applied, EDSMCs replaced collapsible soil elements in the model, enabling the assessment of the geogrid-encased DSMCs' impact on the behaviour of collapsible Sabkha soil under square foundation loads.

2.3 Loading conditions

Fig. 2 depicts the configurations of EDSMCs under foundation loads, showcasing different geometries with varying diameters and spacing distances. The DSMCs were designed with diameters of 0.4 m, 0.6 m, and 0.8 m, and spacing-to-diameter ratios of 2 and 3 were considered. In the study, both untreated and treated collapsible soil with conventional and geogrid-encased DSMCs under saturation conditions were subjected to a load of 200 kN/m². The studied parameters in the analyses include lime percentage,

Table 1 Soil parameters used for the models

Soil	Unsaturated Unit Weight, (kN/m^3)	Saturated Unit Weight, (kN/m^3)	Modulus of elasticity, E (kPa)	Cohesion c' (kPa)	Friction angle, φ' (º)
Non-immersed soil	19.64	21.11	44940	23.80	29.80
Immersed soil	19.64	21.11	5991	0.20	6.80
DSMCs with 5% H. lime under saturation	20.11	21.39	17070	8.97	14.40
DSMCs with 10% H. lime under saturation	20.37	21.45	18140	10.10	16.30
DSMCs with 15% H. lime under saturation	20.80	21.53	18780	10.80	19.80
DSMCs with 20% H. lime under saturation	21.40	21.77	19810	11.20	22.30
Sandy soil	18.00	20.00	15000	3.00	33.00

Table 2 Input parameters of the square foundation

Property	Value
Modulus of Elasticity, *EA* (kPa)	2.1 x 10^7
Thickness (*m*)	0.7
Density, γ (kN/m^3)	25
Poisson's ratio, *v* (-)	0.25

DSMCs diameter, spacing-diameter ratio, and encasement stiffness.

2.4 Machine learning modeling

Various machine learning algorithms can be applied to solve different types of problems. In the context of soil property prediction and optimization, several algorithms is being utilized.

2.4.1 Linear Regression (LR)

LR is a fundamental and widely used ML algorithm for predicting continuous outcomes. It is a supervised learning technique that models the linear relationship between input features and a target variable. In linear regression, the goal is to find the best-fitting line or hyperplane that minimizes the difference between the predicted values and the actual values of the target variable. The algorithm works by estimating the coefficients (slope and intercept) of the linear equation that represents the relationship between the input features and the target variable. The linear regression equation is given by:

$$y = \sum_{i=1}^{n} b_i x_i + b_0 \quad (1)$$

where y is the dependent variable, x_1, x_2,..., x_n are the independent variables, b_0 is the intercept, and b_1, b_2,..., b_n are coefficients that represent the relationship between the independent variables and the dependent variable.

2.4.2 Support Vector Machines (SVM)

SVM is a powerful algorithm for both classification and regression tasks. It constructs a hyperplane that maximally

The linear SVM characteristic equations are listed as follow

$$f(x) = wx + b \quad (2)$$

where w represents the weight vector, x is the input vector, and b is the bias term. The optimized values of w and b can be acquired by minimizing the following term

$$\min \frac{1}{2}\|W\|^2 + C\sum_{i=1}^{N}(\xi_i + \xi_i^*) \quad (3)$$

with the following constraints

$$\begin{cases} y_i - wx_i - b \le \varepsilon + \xi_i \\ wx_i + b - y_i \le \varepsilon + \xi_i^* \\ \xi_i, \xi_i^* \ge 0 \end{cases} \quad (4)$$

where ε indicates an error tolerance, and C is a compromise between the empirical error and the general term.

2.4.3 Gaussian Process Regression (GPR)

GPR is a probabilistic algorithm that can model complex relationships between input features and target variables. It is particularly useful when dealing with limited data points. GPR is employed to predict soil properties by estimating the distribution of possible outcomes, providing valuable insights into uncertainty.

A general purpose function (GP) may be described by its covariance function, k(x,x'), which is the kernel function, and its mean function, m(x), where x and x' are two instances inside the input features matrix x. Consequently, the following is a description of the predicted y* values as a Gaussian process function

$$y^* \sim GP(m(x), k(x, x')) \quad (5)$$

2.4.4 Random Forest (RF)

RF creates an ensemble of decision trees by training multiple trees on different subsets of the data. Each tree in the forest is constructed independently and acts as a "weak learner." During prediction, RF combines the predictions of all trees in the ensemble and takes the average (in regression) or majority vote (in classification) to generate the final prediction. RF is known for its ability to handle high-dimensional data, handle outliers, and reduce overfitting. The equation for the random forest prediction is

$$y = mode(y1, y2, \ldots, yn) \quad (6)$$

where yi stands for each tree's prediction, and mode is the average for regression or the most common prediction for classification.

2.4.5 Decision Tree (DT)

DT algorithm constructs a single tree that recursively partitions the data based on the values of input features. Each internal node represents a test on a feature, and each leaf node represents a predicted outcome. Decision Trees are intuitive and easy to interpret, as they provide clear decision rules. However, they are prone to overfitting and can create complex trees that do not generalize well to unseen data. Both RF and DT have been widely used in predicting soil properties. For example, soil texture, which refers to the relative proportions of sand, silt, and clay in the soil, is to be predicted using these algorithms. By training on a dataset with known soil properties and corresponding input features, such as particle size distribution and organic matter content, RF and DT can learn the patterns and relationships between the features and the soil texture. Similarly, compaction characteristics, such as soil density and porosity, can also be predicted using these algorithms by training on relevant input features like moisture content and compaction effort.

2.4.6 Extreme gradient boosting (XGBoost)

XGBoost is an ensemble method that combines weak models (often decision trees) to improve performance in predicting soil properties like settlement and shear strength. It is highly efficient and accurate, widely used in data science competitions and real-world applications. This optimized implementation of gradient boosting handles regression and classification tasks, sequentially building an ensemble of decision trees to minimize a loss function and correct mistakes. XGBoost excels at capturing both linear and nonlinear relationships by iteratively adjusting weights based on previous trees' errors. It incorporates regularization, tree pruning, and automatic handling of missing values. With tunable hyperparameters, XGBoost is popular for its scalability, speed, and effectiveness in various domains.

2.4.7 Model performance metrics

When evaluating machine learning models, various metrics are used to assess their effectiveness in regression tasks. These metrics include Mean Squared Error (MSE), Root Mean Squared Error (RMSE), Mean Absolute Error (MAE), Coefficient of Determination (R^2-Score), Explained Variance Score (EVS), Mean Percentage Error (MPE), and Median Absolute Error (MedAE). Considering multiple metrics provides a comprehensive understanding of the model's performance. The choice of evaluation metric should align with the specific requirements of the problem. In this study, the R^2-Score was adopted as a powerful metric to evaluate the model's performance. It quantifies the model's ability to explain the variance in the target variable and provides insights into its predictive power and goodness of fit. A high R^2-Score indicates strong performance, while a low score suggests inadequate capture of patterns and variability. The R^2-Score is widely accepted and allows for straightforward comparisons between models, providing a clear measure of performance and it is calculated by

$$R^2 = 1 - \frac{\sum_{i=1}^{N}(y_i - \hat{y}_i)^2}{\sum_{i=1}^{N}(y_i - \bar{y}_i)^2} \quad (7)$$

where $\bar{y}_i$ denotes the mean values of the predicted output.

3. Results and discussion

The primary objective of this study is to improve the performance of end bearing DSMCs under foundation structures. Construction on reinforced saturated collapsible soil with conventional DSMCs poses risks due to weak lateral support from the surrounding collapsible soil. To address this issue, the current study utilizes EDSMCs in reinforcing collapsible soil under the same foundation load of 200 kPa.

3.1 Reinforced Sabkha soil with geogrid EDSMCs

The utilization of geogrid materials with varying axial stiffness values as encasements significantly enhances the lateral support provided to DSMCs. In Fig. 3, the relationship between applied load and settlement/foundation width is illustrated. When untreated saturated collapsible soil is loaded, it exhibits low ultimate bearing capacity and experiences considerable settlement even at lower applied loads.

Introducing conventional DSMCs for soil reinforcement increases the ultimate bearing capacity up to three times. However, this method may not be practical, especially under higher loads. By encasing DSMCs with geogrid possessing a stiffness of 800 kN/m, there is a substantial improvement in bearing capacity and a notable decrease in settlement, evident across various lime percentages, diameters, and spacing distances as shown in Figs. 3(a) to 3(j). As the stiffness of the encasement increases, there is a further enhancement in bearing capacity and a more significant reduction in settlement due to the robust lateral support provided by the geogrid encasement. Reinforced saturated soil with EDSMCs featuring a geogrid stiffness of 5000 kN/m exhibits smaller settlement compared to lower stiffness values across all cases studied. Similarly, soil reinforced with a geogrid stiffness of 10,000 kN/m demonstrates the smallest settlement values among all cases, with the least settlement occurring at higher geogrid stiffness, increased lime content, and area replacement ratios. The study reveals that there are reductions in the maximum settlement values as the lime content in the EDSMCs increases. This reduction rate is more significant at a geogrid stiffness value of 800 kN/m, as shown in Fig. 4.

On the other hand, the reinforced soil with EDSMCs of 10,000 kN/m stiffness induces lower settlement values compared to the case with an encasement stiffness of 800 kN/m. The greatest reduction in settlement occurs with higher encasement stiffness and lime content among the studied cases.

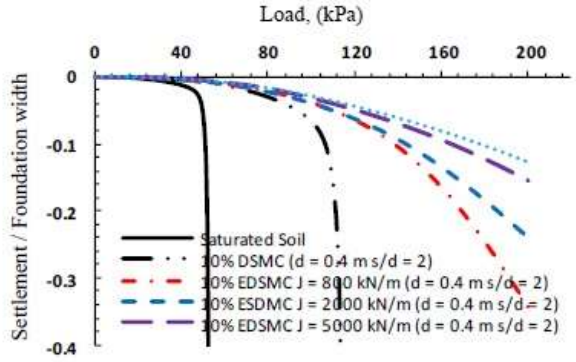

(a) Series A-2

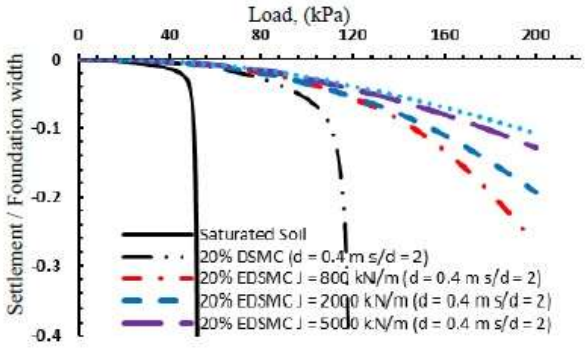

(b) Series A-4

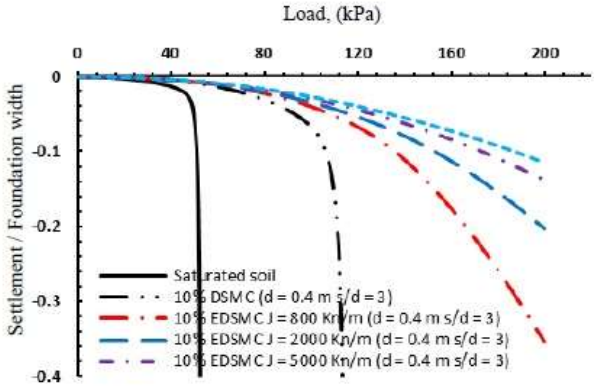

(c) Series B-2

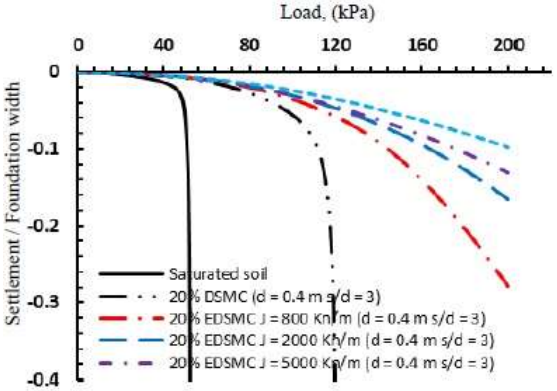

(d) Series B-4

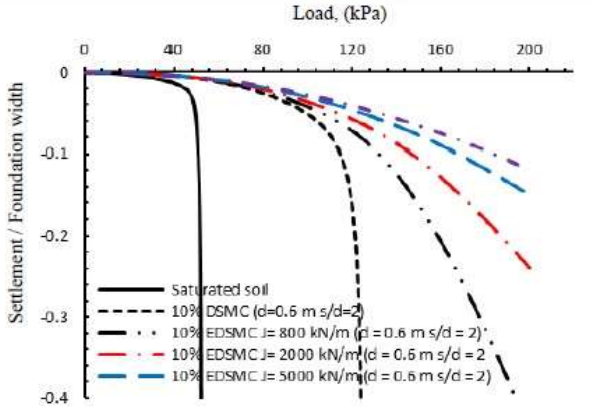

(e) Series C-2

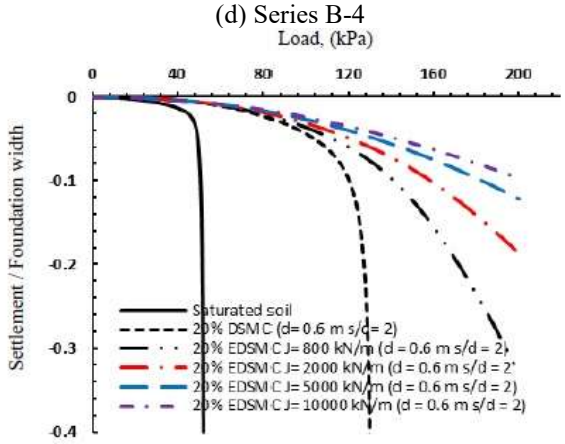

(f) Series C-4

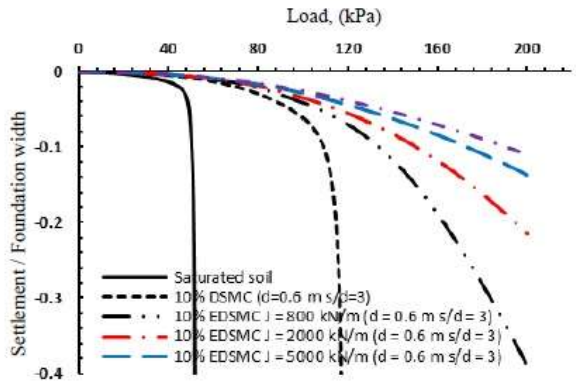

(g) Series D-2

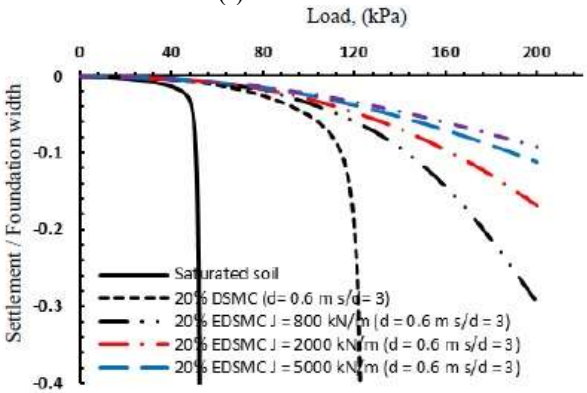

(h) Series D-4

Fig. 3 Load-settlement relationships under the same load of 200 kPa for encased DSMCs with different encasement stiffness values, lime contents, diameters and spacing distances (a, b, c, d, e, f, g, h, i and j)

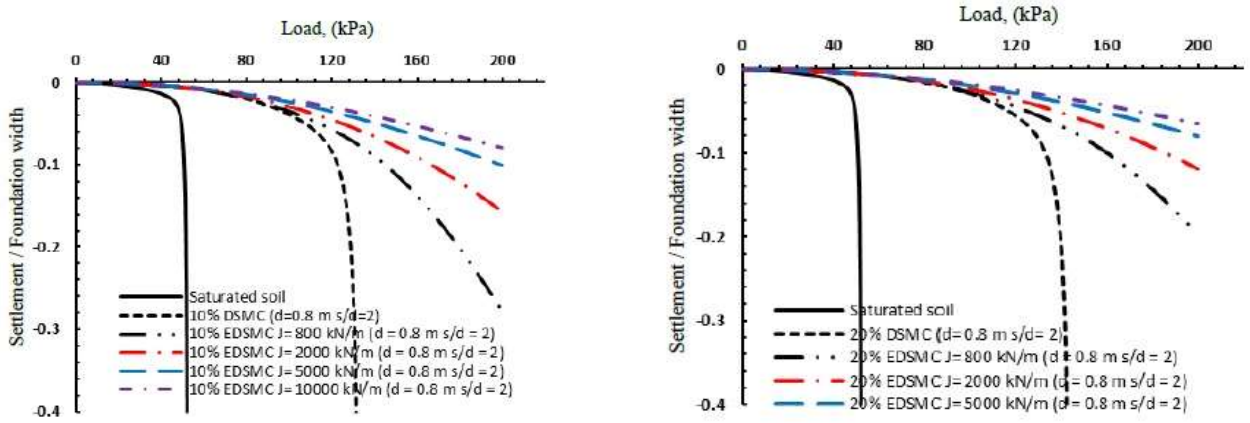

(i) Series E-2 (j) Series E-4

Fig. 3 Continued-

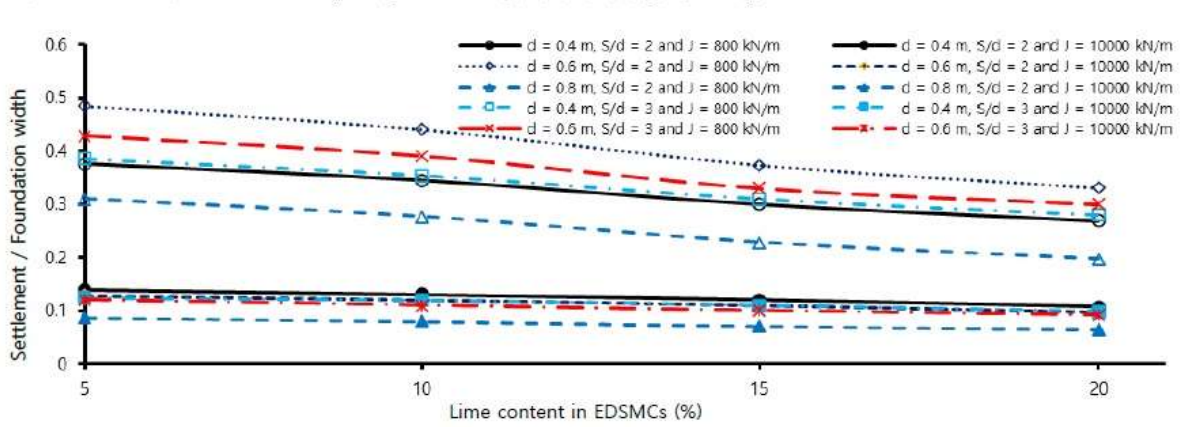

Fig. 4 Effect of EDSMC lime content on the settlement control

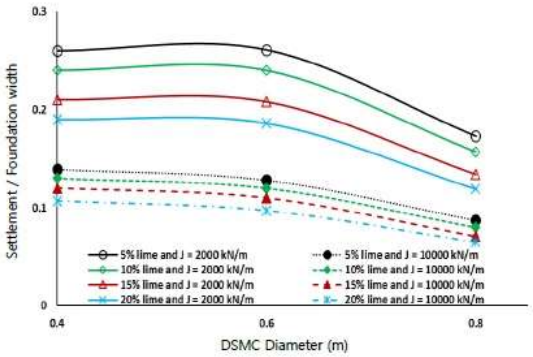

Fig. 5 Effect of EDSMC diameter on the settlement control

Regarding the diameter of the EDSMCs, there is a slight reduction in settlement as the diameter increases from 0.4 to 0.6 m, which is more pronounced at an encasement stiffness of 2000 kN/m, as indicated in Fig. 5. However, the settlement reduction rate is greater when the diameter increases from 0.6 m to 0.8 m at different lime contents, especially when using an encasement stiffness of 2000 kN/m. This might be attributed to the influence of area replacement ratio of EDSMCs.

The encasement of DSMCs causes a significant reduction in the foundation settlement. The settlement decrement continues with increasing geogrid stiffness for the different study cases, as depicted in Fig. 6. The settlement reduces effectively when increasing geogrid stiffness from 800 kN/m to 2000 kN/m.

Beyond the later value, the settlement decrement rate reduces when increasing geogrid stiffness from 2000 kN/m to 5000 kN/m. The last increment of geogrid stiffness from 5000 kN/m to 10 000 kN/m induces the smallest settlement reduction rate as shown in Figs. 6(a)-6(c).

In the following sections, the foundation vertical displacement, vertical effective stress and loads in EDMCS and in soil, and the EDSMCs lateral bulging were analyzed

for EDSMCs with diameters of 0.4 m and 0.8 m, a spacing ratio of 2, and 20% lime content using geogrid encasement stiffness of 800 kN/m and 10,000 kN/m for each case under a load of 200 kPa.

3.1.1 Foundation settlement of the reinforced sandy Sabkha soil with EDSMCs

The distribution of vertical displacement was found to be similar for all cases, with the maximum settlement occurring under the centerline of the foundation and

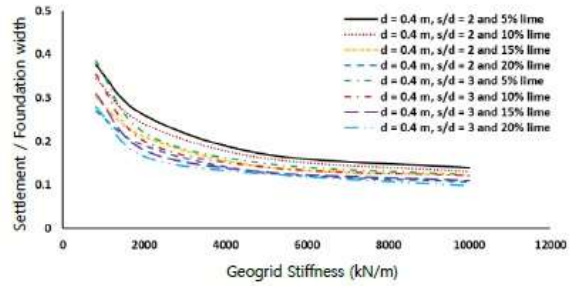

(a) d = 0.4 m

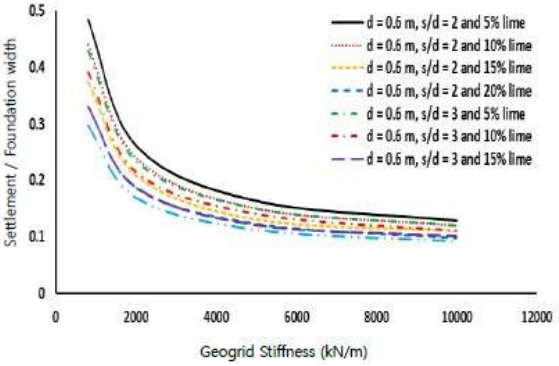

(b) d = 0.6 m

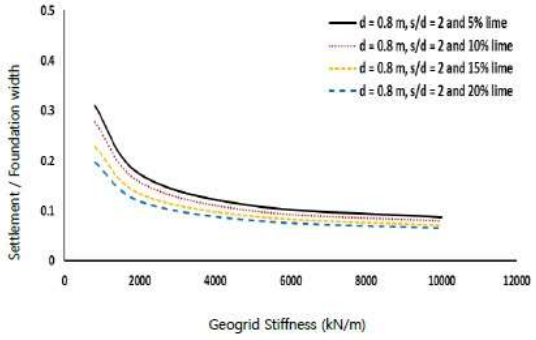

(c) d = 0.8 m

Fig. 6 Effect of encasement stiffness on the settlement control for diameters of (a)-(d) = 0.4 m, (b)-(d) = 0.6 m and (c)-(d) = 0.8 m

decreasing towards the edges. Settlement decreases rapidly beyond, reaching near-zero values at 2.2 m from the centerline.

For all cases except EDSMCs with diameters of 0.4 m and 0.8 m using an encasement stiffness of 800 kN/m, settlement approaches zero with increasing horizontal distance from the centerline. These two cases exhibits upward vertical displacement at far distances, indicating sustained high settlement. This behaviour is more pronounced for the 0.4 m diameter and 800 kN/m stiffness case. When geogrid stiffness is increased to 10,000 kN/m for EDSMC, significant settlement reductions are observed as illustrated in Fig. **7.** Additionally, EDSMCs with a diameter of 0.8 m show less settlement compared to the 0.4 m diameter. Therefore, using EDSMCs with a high stiffness of 10,000 kN/m in collapsible soil effectively minimizes foundation settlement and eliminates upward vertical displacement, enhancing foundation performance.

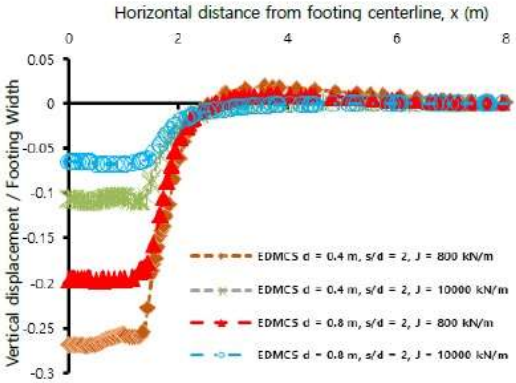

Fig. 7 Vertical displacement distribution of EDSMCs directly under the footing under a load of 200 kN/m^2

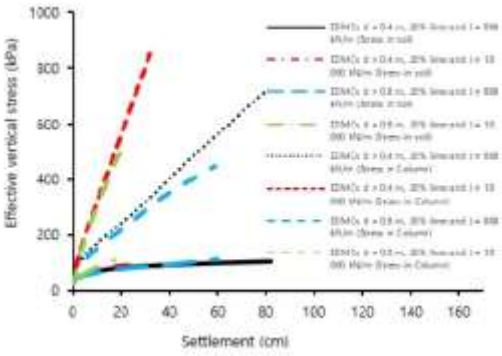

(a)

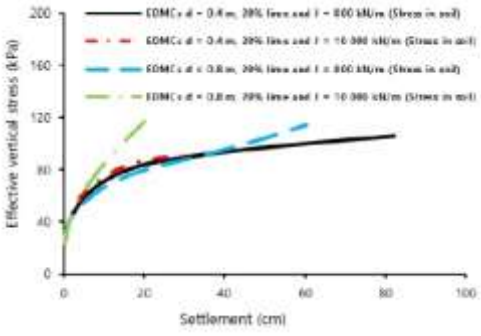

(b)

Fig. 8 (a) Vertical effective stress in the top of soil and EDMSCs under a foundation load of 200 kPa and (b) Vertical effective stress in the top of soil surrounding EDMSCs under a foundation load of 200 kPa

3.1.2 Stress and load sharing in the reinforced sandy Sabkha soil with EDSMCs

The evolution of effective vertical stress in EDSMCs and the soil with settlement is relatively consistent for both diameters at both encasement stiffness levels, as demonstrated in Figs. 8(a) and 8(b). The vertical stress in EDSMCs exhibits a linear relationship along settlement development, with EDSMCs having a higher encasement stiffness inducing greater effective stress. Conversely, the surrounding soils display elasto-plastic behaviour, more pronounced at lower encasement stiffness values.

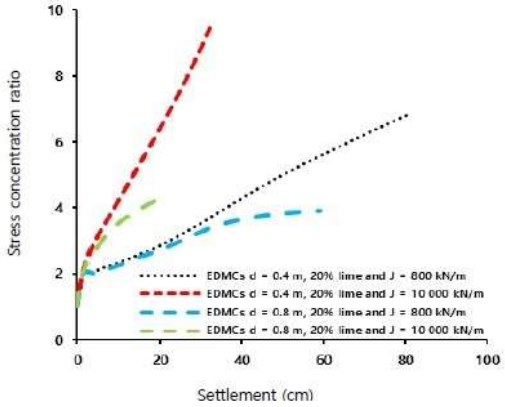

Fig. 9 Stress concentration ratio in EDMSCs under a foundation load of 200 kPa

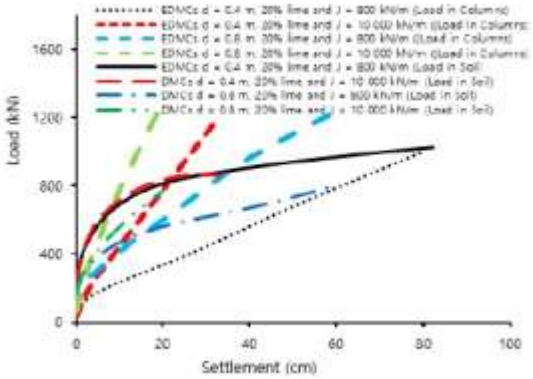

Fig. 10 Loads carried by the soil and EDMSCs during a foundation loading to 200 kPa

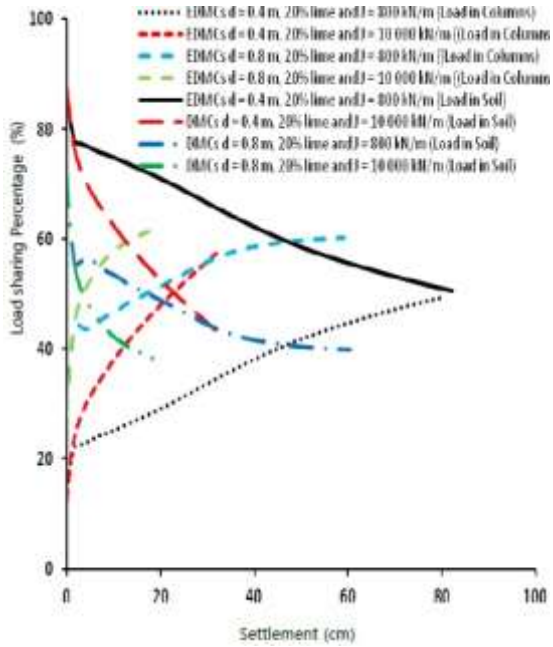

Fig. 11 Load sharing-settlement development in the soil and EDMSCs during a foundation loading to 200 kPa

This study found that EDSMCs bear more stress compared to the surrounding soil. Increasing the encasement stiffness from 800 kN/m to 10,000 kN/m leads to significant stress increments in the columns and the stress concentration ratio, along with some increases in the stress of the surrounding soils, as depicted in Figs. 8 and 9. Fig. 9 also highlights that the stress concentration ratio in EDSMCs with a diameter of 0.4 m is higher than that of EDSMCs with a diameter of 0.8 m. This is attributable to the area replacement ratio of EDSMCs with d = 0.4 m is smaller than that of EDSMCs with d = 0.8 m. To calculate the load carried by EDSMCs, due to the above reason, the average effective vertical stress in them was multiplied by their areas. Similarly, the load carried by the surrounding soil was computed by multiplying its area by the average effective vertical stress within it. In cases where EDSMCs with a diameter of 0.4 m and an encasement stiffness of 800 kN/m are used, the soil carries a greater load than the EDSMCs at lower settlement values. However, this difference decreases with increasing settlement. At the highest settlement value, the soil carries a greater load.

A similar trend is observed when using EDSMCs with a diameter of 0.4 m and an encasement stiffness of 10,000 kN/m, except that the EDSMCs carries a greater load at higher settlement values as depicted in Fig. 10.

In contrast, employing EDSMCs with a diameter of 0.8 m leads to an increase in the load carried by the columns and a decrease in the load carried by the soil. Further increases in loads are observed in EDSMCs and additional load reductions in the surrounding soil when the encasement stiffness is raised from 800 kN/m to 10,000 kN/m.

The load-sharing development between EDSMCs and the surrounding Sabkha soil under a foundation load of 200 kPa is illustrated in Fig. 11. Across all cases, the loads in EDSMCs increase with settlement, while the opposite is true for the loads in the surrounding soil. Hence, as applied loads and settlement increase, the loads transfer from the soil to the EDSMCs. At higher settlement values, EDSMCs carries greater loads than the surrounding soil, except for the case of EDSMCs with a diameter of 0.4 m and an encasement stiffness of 800 kN/m.

Overall, increasing the diameter and encasement stiffness of EDSMCs results in significant load increments in the columns and substantial load reductions in the surrounding soil, as depicted in Table 3 and Fig. 11. Therefore, utilizing EDSMCs in collapsible soil with a diameter of 0.8 m and an encasement stiffness of 10,000 kN/m increases the load transferred to the EDSMCs, carrying 62.3% of the applied load.

3.1.3 Lateral bulging of DSMCs in sandy collapsible Sabkha soil

The lateral bulging behaviour of EDSMCs was analyzed to understand how the geogrid encasement stiffness influences the lateral support provided by the surrounding soil. For the 0.4 m diameter columns, lateral bulging was examined for central, edge, and corner EDSMCs. The central columns exhibits uniform lateral bulging, while the edge columns bulge externally, and the corner columns induce diagonal external bulging as illustrated in Fig. 12.

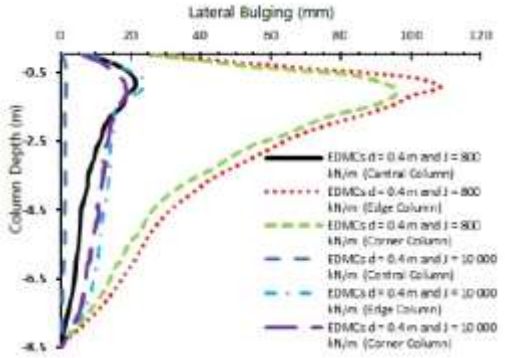

(a)

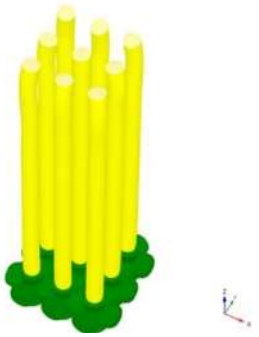

(b)

Fig. 12 (a) Lateral bulging of EDMSCs under a foundation load of 200 kPa (d = 0.4 m and L = 20%) and (b) Overall Lateral bulging of EDMSCs (d = 0.4 m, L = 20% and J = 10 000 kN/m)

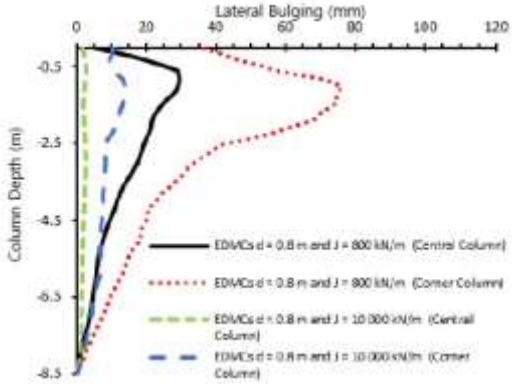

(a)

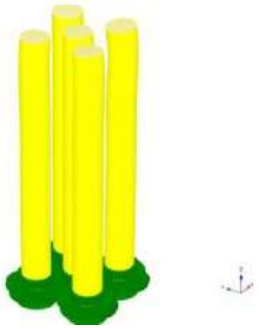

(b)

Fig. 13 (a) Lateral bulging of EDMSCs under a foundation load of 200 kPa (d = 0.8 m and L = 20%) and (b) Overall Lateral bulging of EDMSCs (d = 0.8 m, L = 20% and J = 10 000 kN/m)

Table 3 loads sharing percentages between EDSMCs and the surrounding soil

Case	% Load carried by EDSMCs	% Load carried by soil
d = 0.4 m and J = 800 kN/m	49..5	50.5
d = 0.4 m and J = 10 000 kN/m	57.5	42.5
d = 0.8 m and J = 800 kN/m	60.2	39.8
d = 0.8 m and J = 10 000 kN/m	62.3	37.7

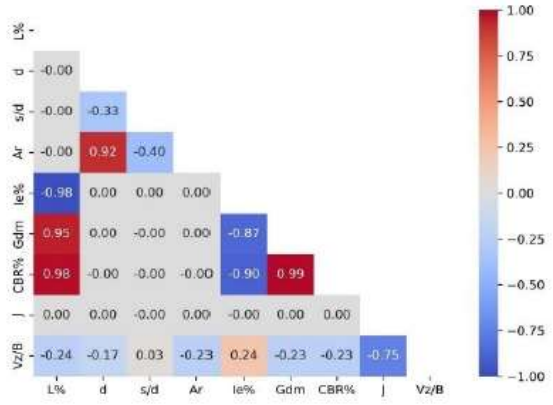

Fig. 14 Correlation matrix of various soil parameters presents the correlation coefficients between different pairs of variables

Maximum bulging typically occurs at a depth of around 1.0 m, with edge columns experiencing the greatest bulging and Central columns the least. With a geogrid encasement stiffness of 800 kN/m, the lateral bulging reaches a peak of 108 mm at the edge column, indicating a reduction in bearing capacity due to this lateral movement. Increasing the encasement stiffness to 10,000 kN/m leads to a significant decrease in lateral bulging for all EDSMCs types (central, edge or corner), as shown in Figs. 12(a) and 12(b).

For the 0.8 m diameter columns, lateral bulging was assessed for central and corner EDSMCs under a load of 200 kPa as depicted in Fig. 13(a). Corner columns exhibit diagonal bulging, while central columns show uniform bulging as shown in Fig. 13(b). The larger diameter columns display lower lateral bulging compared to the 0.4 m diameter columns at both geogrid stiffness levels. The lateral bulging extends throughout the depth of the columns, transferring stress to lower sections due to the increased stiffness of the EDSMCs at this diameter. Overall, the study highlighted that increasing the geogrid encasement stiffness led to a substantial reduction in lateral bulging for both 0.4 m and 0.8 m diameter EDSMCs. This reduction in lateral movement is crucial for enhancing bearing capacity and minimizing settlement in collapsible soils. By providing strong lateral support, the EDSMCs effectively transfer stress downwards, enabling them to function efficiently as piles in such challenging soil conditions.

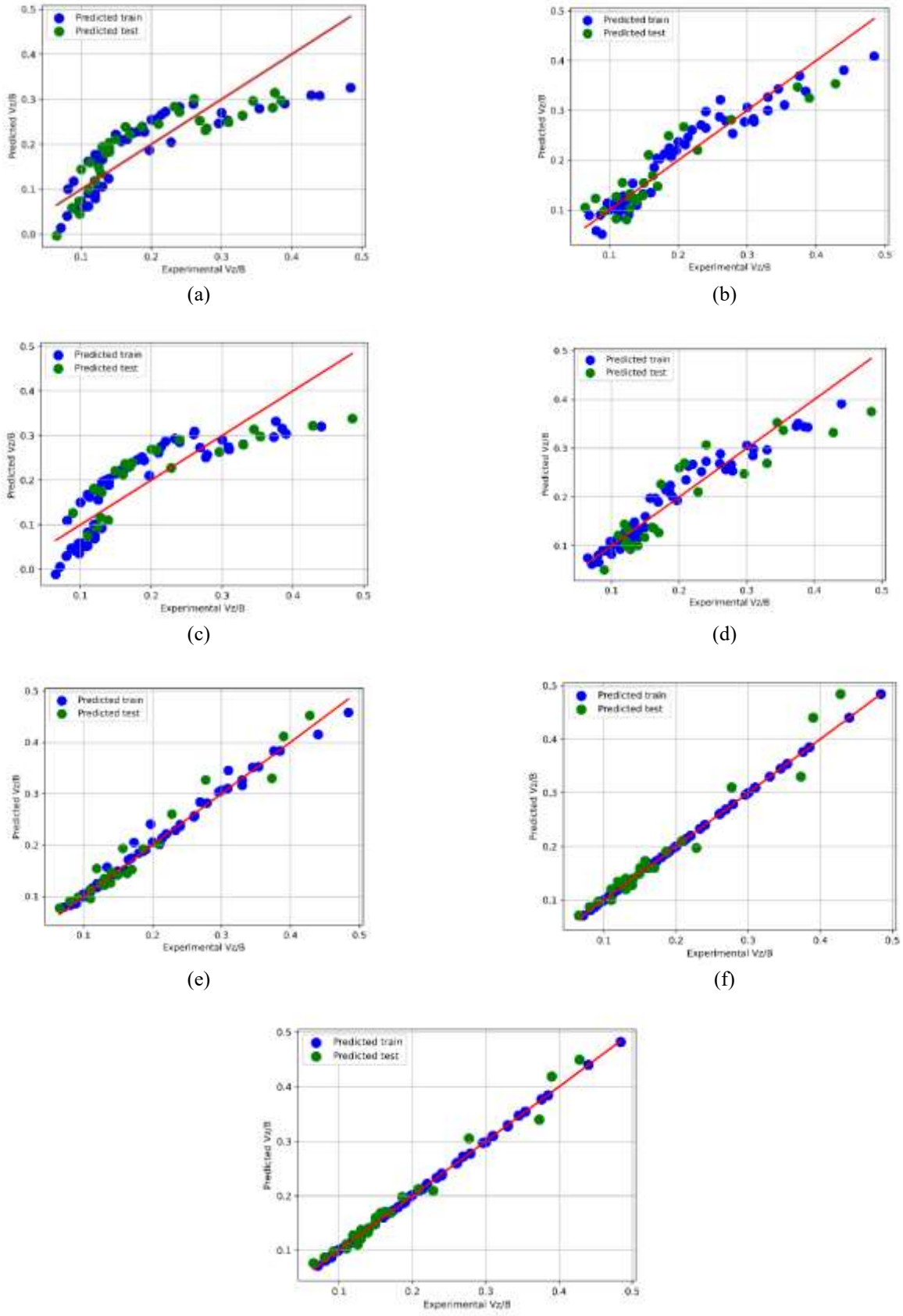

Fig. 15 Predicted versus Experimental *Vz/B* modeled using various ML algorithms: (a) LR, (b) NLR, (c) SVM, (d) GPR, (e) RF, (f) DT, and (g) XGBoost

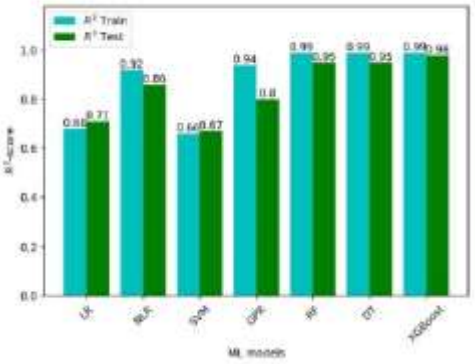

Fig. 16 Multiple ML algorithms utilized to evaluate models performance on both the training and testing datasets, employing R^2-Score metric

3.2 Machine learning analyses results for Reinforced Sabkha soil with encased DSMCs

The output of the ML analyses is the maximum settlement to foundation width ratio (Vz/B), calculated under applied loads of 200 kPa for all the studied cases. The correlation matrix in Fig. 14 shows the correlation coefficients between different pairs of variables, providing insights into the relationships between the various soil parameters. In general, all studied features are negatively correlated with Vz/B, except for the spacing-to-diameter ratio (s/d) and the collapse index (I_e). The encasement stiffness (J) has the greatest influence parameter in reducing settlement under applied loads, with a correlation coefficient of -0.75. Parameters such as lime content, area replacement ratio, maximum dry density, CBR and the collapse index (I_e) have approximately the same effect in reducing settlement, accounting for about one-third of the encasement stiffness influence. Moreover, the diameter of the EDSMCs has a smaller influence in reducing settlement, acting about one-fifth of the influence of encasement stiffness. Lastly, the spacing distances between EDSMCs have a slight effect on foundation settlement. Therefore, the encasement and its stiffness are the most influential parameters in determining settlement values. The existence of the encasement around DSMCs weakens the role and influence of the other parameters studied. This provides strong evidence of the important role of EDSMCs in effectively improving foundations performance on saturated collapsible sandy Sabkha soil, as indicated by the numerical analyses results. The ML models analyses confirm the above-mentioned results of the numerical analyses and provide a deeper understanding of the role of EDSMCs in enhancing the behaviour of saturated collapsible sandy Sabkha soil.

Fig. 15 displays scatter plots comparing the predicted and actual qu values modeled using a range of ML algorithms such as LR, NLR, SVM, GPR, RF, DT, and XGBoost. These scatter plots provide a visual representation of how well each ML algorithm captures the relationship between the predicted and calculated V_z/B values. This analysis enables us to assess the accuracy and performance of the models across the various algorithms. By examining the scatter plots in Fig. 16, we can gain valuable insights into the effectiveness of each ML algorithm in accurately predicting the Vz/B values and understand how they compare to the numerical results data. Fig. 15 provides an evaluation of model performance for various ML algorithms on both the training and testing datasets, using the R^2-Score as a metric. Analyzing the training results in Fig. 16, we observe that all models performed well, with R^2-Scores ranging from 0.66 to 0.99. These high R^2-Scores indicate that the ML algorithms effectively captured the patterns and relationships present in the training dataset. The models' strong performance on the training data suggests their ability to accurately predict the target variable and their capability to fit the observed data closely. Moving on to the testing set results, we see that the R^2-Scores range from 0.67 to 0.98. These scores demonstrate that the models' predictive performance is also strong on the testing set. While there is some variation in the performance among the models, with lower R^2-Scores indicating relatively weaker performance compared to the training set, the models still exhibit a good ability to generalize and predict the target variable accurately on unseen data. Fig. 16 shows that RF, DT, and XGBoost achieved high R^2-Scores of 0.95, 0.95, and 0.98, respectively. These scores indicate that these models effectively captured patterns and relationships in the training data, demonstrating strong predictive performance. They showcase the ability of RF, DT, and XGBoost to accurately predict the target variable and generalize well to unseen data. These results highlight the effectiveness of the ML algorithms in capturing the underlying patterns in the data and their potential for reliable predictions in real-world applications.

4. Conclusions

The numerical analyses of full-scale 3D models focused on untreated and treated collapsible sandy Sabkha soil with EDSMCs under square foundation loads. Various parameters such as EDSMCs configurations, lime content, area replacement ratio and geogrid stiffness were considered. Advanced machine learning models were applied to numerical study, incorporating features such as EDSMCs collapse index, maximum dry unit-weight, and CBR, in addition to the parameters used in the numerical analysis. The findings are as follows:

- The encasement of DSMCs in saturated collapsible soil significantly enhances the foundation's performance by increasing its bearing capacity and reducing settlement. The improvement in settlement control increases with higher lime content, area replacement ratio, and encasement stiffness. The greatest reduction in settlement was observed when using EDSMCs with a diameter of 0.8 m, spacing ratio of 2, lime content of 20%, and geogrid stiffness of 10,000 kN/m.
- The substantial improvement in foundation performance enables the safe construction of private structures and infrastructure on reinforced saturated collapsible Sabkha soil with EDSMCs. The higher

encasement stiffness provides strong lateral support to the DSMCs, minimizing lateral bulging, facilitating stress transfer to columns acting as piles and increasing effectively loads sharing by EDSMCs.

- ML analyses revealed that the most influential feature is the encasement stiffness in reducing foundation settlement, decreasing the role of other studied features. Most of the ML models performed well in accurately predicting the parameters of reinforced Sabkha soil, with R^2-Scores exceeding 0.95 for the testing dataset. These high scores indicate good prediction performance and effectiveness in capturing soil features. The ML models also confirmed the important role of DSMCs encasement, aligning well with the results of the numerical study.

Acknowledgments

The authors extend their appreciation to the Deputyship for Research & Innovation, Ministry of Education in Saudi Arabia for funding this research work through the project number (0222-1443-S).

References

A Rashid, A.S., Bunawan, A.R. and Mat Said, K.N. (2017), "The deep mixing mMethod: Bearing capacity studies", *Geotech. Geol. Eng*., **35**, 1271-1298. https://doi.org/10.1007/s10706-017-0196-x.

Abas, H.A., Alluqmani, A.E. and Yousif, I. (2024), "Assessing deep soil mixing for excavation support in Sabkha soils: A numerical study", *J. Umm Al-Qura Univ. Eng. Archit*., **15**, 1-13. https://doi.org/10.1007/s43995-023-00036-y.

Abbey, S. and Ngambi, S. (2015), "Understanding the performance of deep mixed column improved soils-a review", *Int. J. Civil Eng. Technol*., **6**, 97-117.

Al-Amoudi, O.S.B. (2002), "Characterization and chemical stabilization of Al-Qurayyah Sabkha soil", *J. Mater. Civil Eng*., **14**(6), 478-484. https://doi.org/10.1061/(ASCE)0899-1561(2002)14:6(478).

Al-Amoudi, O.S.B. and Abduljauwad, S.N. (1995), "Strength characteristics of Sabkha soils", *Geotech. Eng. J*., **26**(1), 73-92.

Alawaji, H.A. (1998), "Model plate-load tests on collapsible soil", *J. King Saud Univ. – Eng. Sci*., **10**(2), 255-269. https://doi.org/10. 1016/S1018-3639(18)30700-1.

Alhamdi, M.K. and Albusoda, B.S. (2021), "A review on deep mixing method for soil improvement", *IOP Conf. Ser.: Mater. Sci. Eng*., **1105**, 012110. https://doi.org/10.1088/1757-899X/1105/1/012110

Alnunu Mahdi, Z. and Nalbantoglu, Z. (2022), "Laboratory analysis of loose sand mixed with construction waste material in deep soil mixing", *Geomech. Eng*., **28**(6), 559-571. https://doi.org/10.12989/gae.2022.28.6.559.

Al-Obaidy, N., Jefferson, I. and Ghataora, G. (2015), "Treatment of Iraqi collapsible soil using encased stone columns", *Proceedings of the 15th Asian Regional Conference on Soil Mechanics and Geotechnical Engineering*, ARC 2015, Fukuoka, Kyushu, Japan. https://doi.org/10.3208/jgssp.IRQ-01.

Alnunu, M.Z. and Nalbantoglu, Z. (2021), "Performance of using waste marble dust for the improvement of loose sand in deep soil mixing", *Arabian J. Sci. Eng*., **47**(4), 4681-4694. https://doi.org/10.1007/s13369-021-06252-9.

Al-Rawas, AA. (2000), "State-of-the-art review of collapsible soils", *Sci. Technol. Rev*., **5**(2), 115-135. https://doi.org/10.24200/squjs.vol5iss0pp115-135.

Alrubaye, A.J., Hasan, M. and Fattah, M.Y. (2016), "Engineering properties of clayey soil stabilized with lime", *ARPN J. Eng. Appl. Sci*., **11**, 2434-2441.

Araujo, G., Palmeira, E. and Cunha, R. (2009), "Behaviour of geosynthetic-encased granular columns in porous collapsible soil", *Geosynth. Int*.**,** **16**(6),433-451. https://doi.org/10.1680/gein.2009.16.6.433.

Ayadat, T. and Hanna, A. (2005), "Encapsulated stone columns as a soil improvement technique for collapsible soil", *Proceedings of the ICE - Ground Improvement*, **9**(4), 137-147. https://doi.org/10.1680/grim.2005.9.4.137.

Ayadat, T., Hanna, A. and Etezad, M. (2008), "Failure process of stone columns in collapsible soils", *IJE Trans. B: Appl*., **21**(2), 135-142.

Bahmyari, H., Ajdari, M., Vakili, A. and Ahmadi, M.H. (2021), "The role of the cement, lime, and natural pozzolan stabilizations on the mechanical response of a collapsible soil", *Transport. Infrastruct. Geotechnol*., **8**, 452-472. https://doi.org/10.1007/s40515-020-00146-3.

Bahrami, M. and Marandi, S. (2021), "Large-scale experimental study on collapsible soil improvement using encased stone columns", *Int. J. Eng*., **34**(5), 1145-1155. https://doi.org/10.5829/ije.2021.34.05b.08.

Bouassida, M., Fattah, M.Y. and Mezni, N. (2020), "Bearing capacity of foundation on soil reinforced by deep mixing columns", *Geomech. Geoeng*., **17**(1), 309-320. https://doi.org/10.1080/17486025.2020.1755458.

Bouassida, M., Fattah, M.Y. and Mezni, N. (2022), "Bearing capacity of foundation on soil reinforced by deep mixing columns", *Geomech. Geoeng*., **17**, 309-320. https://doi.org/10.1080/17486025.2020.1755458.

Clemence, S. and Finbarr, A. (1981), "Design considerations for collapsible soils", *Geotech. Eng. Div. ASCE*, **107**(3), 305-317. https://doi.org/10.1061/AJGEB6.0001102.

Derbyshire E. (2001), "Geological hazards in loess terrain, with particular reference to the loess regions of China", *Earth. Sci. Rev*., **54**(1-3), 231-260. https://doi.org/10.1016/S0012-8252(01)00050-2.

Dinarvand, R. and Ardakani, A. (2022), "Shear behavior of geotextile-encased gravel columns in silty sand-Experimental and SVM modeling", *Geomech. Eng*., **28**(5), 505-520. https://doi.org/10.12989/gae.2022.28.5.505.

Disfani, M.M., Mohammadinia, A., Arulrajah, A., Horpibulsuk, S. and Leong, M. (2021)., "Lightly stabilized loose sands with Alkali-activated fly ash in deep mixing applications", *Int. J. Geomech*., **21**(3), https://doi.org/10.1061/(ASCE)GM.1943-5622.000195.

Ebrahimi, M., Eslami, A., Hajirasouliha, I., Ramezanpour, M. and Pilakoutas, K. (2023), "Effect of ceramic waste powder as a binder replacement on the properties of cement-and lime-based mortars", *Constr. Build. Mater*., **379**, 131146. https://doi.org/10.1016/j.conbuildmat.2023.131146.

Elsawy, M.B.D. and El-Garhy, B. (2017), "Performance of granular piles-improved soft ground under raft foundation: A numerical study", *Int. J. Geosynth. Ground Eng*., **3**(36). https://doi.org/10.1007/s40891-017-0113-7.

Elsawy, M.B.D. and Lakhouit, A. (2021), "Geotechnical behaviour of sandy Sabkha soils based on experimental and numerical iInvestigations", *Indian Geotech. J*., 1-16. https://doi.org/10.1007/s40098-021-00555-2.

Elsawy, M.B.D. and Lakhouit, A., (2023), "Enhancing mechanical characteristics of a collapsible sandy Sabkha soil using an eco-friendly admixture: An experimental and numerical study", *Int. J. Geotech. Eng*., **17**(2), 124-139.

https://doi.org/10.1080/19386362.2023.2182967.
Esmaeili, M. and Khajehei, H. (2016), "Mechanical behaviour of embankments overlying on loose subgrade stabilised by deep mixed columns", *J. Rock Mech. Geotech. Eng*., **8**(5), 651-659. https://doi.org/10.1016/j.jrmge.2016.02.006.
Feda, J. (1988), "Collapse of loess upon wetting", *Eng. Geol*., **25**(2-4), 263-269.
Gaaver, K.E.(2012), "Geotechnical properties of Egyptian collapsible soils", *Alexandria Eng. J*., **51**(3), 205-210. https://doi.org/10.1016/j.aej.2012.05.002.
Hammad, M.A., Mohamedzein, Y. and Al-Aghbari, M. (2023), "Improving the properties of saline soil using a deep soil mixing technique", *Civil Eng*., **4**, 1052-1070. https://doi.org/10.3390/civileng4040057.
Houston, S.L., Houston, W.N. and Spadola, D.J. (1988), "Prediction of field collapse of soils due to wetting", *J. Geotech. Eng.*, **114**(1), https://doi.org/10.1061/(ASCE)0733-9410(1988)114:1(40).
Houston, S.L., Houston, W.N., Zapata, C.E. and Lawrence, C. (2001), "Geotechnical engineering practice for collapsible soils", *Geotech. Geol. Eng*., **19**(3), 333-355. https://doi.org/10.1023/A:1013178226615.
Ismael, N.F. (1993), "Laboratory and field leaching tests on coastal salt-bearing soils", *J. Geotech. Eng*., **119**(3), 453-470. https://doi.org/10.1061/(ASCE)0733-9410(1993)119:3(453).
Jaiswal, A. and Kumar, R. (2022), "Finite element analysis of granular column for various encasement conditions subjected to shear load", *Geomech. Eng*., **29**(6), 645-655. https://doi.org/10.12989/gae.2022.29.6.645.
Jung, C., Ceglarek, R., Clauvelin, T., Ayeldeen, M. and Kim, D. (2020), "Deep soil mixing in Sabkha soils for foundation support in united Arab Emirates", *Int. J. Geosynth. Ground Eng*., **6**(1), 1-15. https://doi.org/10.1007/s40891-020-0188-4.
Kang, S.H., Kwon, Y.H., Hong, S.G., Chun, S. and Moon, J. (2019), "Hydrated lime activation on byproducts for eco-friendly production of structural mortars", *J. Cleaner Product*., **231**, 1389-1398. https://doi.org/10.1016/j.jclepro.2019.05.313.
Larsson, S. (2003), Mixing processes for ground improvement by deep mixing. Byggvetenskap.
Lawal, A.I. and Kwon**,** S. (2023), "Development of mathematically motivated hybrid soft computing models for improved predictions of ultimate bearing capacity of shallow foundations", *J. Rock Mech. Geotech. Eng*., **15**(3), 747-759.
Liu, Y. and Liang, Y. (2024), "Integrated machine learning for modeling bearing capacity of shallow foundations", *Sci. Rep*., **14**, 8319. https://doi.org/10.1038/s41598-024-58534-5.
Liu, G., Zhang, C., Zhao, M., Guo, W. and Luo, Q. (2020), "Comparison of nanomaterials with other unconventional materials used as additives for soil improvement in the context of sustainable development: A review", *Nanomater*., **11**(1), 15. https://doi.org/10.3390/nano11010015.
Liu, S., Zhang, D., Song, T., Zhang, G. and Fan, L. (2022), "A method of settlement calculation of ground improved by floating deep mixed columns based on laboratory model tests and finite element analysis", *Int. J. Civ. Eng*., **20**, 207-222. https://doi.org/10.1007/s40999-021-00662-4.
Liu, Y., Jiang, Y.J., Xiao, H. and Lee, F.H. (2016), "Determination of representative strength of deep cement-mixed clay from core strength data", *Géotechnique*, **67**(4), 350-364. https://doi.org/10.1680/jgeot.16.P.105.
Lommler, J.C. and Bandini, P. (2015), "Characterization of collapsible soils", *Proceedings of the IFCEE, San Antonio, Texas*.
Mahmoodi, K., Motlagh, N.M. and Ardakani, A.R.M. (2024), "An investigation into the effects of lime-stabilization on soil-geosynthetic interface behavior", *Geomech. Eng*., **38**(3), 231-247. https://doi.org/10.12989/gae.2024.38.3.231.
Makusa, G.P. (2013), Soil stabilization methods and materials in engineering practice: State of the art review.
Nguyen, B., Takeyama, T. and Kitazume, M. (2016), "Internal failure of deep mixing columns reinforced by a shallow stabilized soil beneath an embankment", *Int. J. Geosynth. Ground Eng*., **2**(30). https://doi.org/10.1007/s40891-016-0072-4.
Nouaouria, M.S., Guenfoud, M. and Lafifi, B. (2008), "Engineering properties of loess in Algeria", *Eng. Geol*., **99**(1-2), https://doi.org/10.1016/j.enggeo.2008.01.013.
Pakbaz, M.S. and Farzi, M. (2015), "Comparison of the effect of mixing methods (dry vs. wet) on mechanical and hydraulic properties of treated soil with cement or lime", *Appl. Clay Sci*., **105-106**, 156-169. https://doi.org/10.1016/j.clay.2014.11.040.
Peng, J.B., Sun, P. and Li, X. (2006), "Ground fissure: The major geological and environmental problem in the development of Xi'an City, China", *Environ. Sci. Technol*., **2**, 469e74.
Pereira, L., Godinho, L. and Branco, F.G. (2023), "Predicting unconfined compression strength and split tensile strength of soil-cement via artificial neural networks", *Geomech. Eng*., **33**(6). 611-624. https://doi.org/10.12989/gae.2023.33.6.611.
Phien-wej, N., Pientong, T. and Balasubramaniam, A.S. (1992), "Collapse and strength characteristics of loess in Thailand", *Eng. Geol*., **32**(1-2), 59-72. https://doi.org/10.1016/0013-7952(92)90018-T.
Pourakbar, S. and Huat, B.K. (2017), "A review of alternatives traditional cementitious binders for engineering improvement of soils", *Int. J. Geotech. Eng*., **11**, 206-216. https://doi.org/10.1080/19386362.2016.1207042.
Raja, M.N.A. and Shukla, S.K. (2021), "Predicting the settlement of geosynthetic-reinforced soil foundations using evolutionary artificial intelligence technique", *Geotext. Geomembranes*, **49**(5), 1280-1293. https://doi.org/10.1016/j.geotexmem.2021.04.007.
Raja, M.N.A., Jaffar, S.T.A., Bardhan, A. and Shukla, S.K. (2023), "Predicting and validating the load-settlement behaviour of large-scale geosynthetic-reinforced soil abutments using hybrid intelligent modeling", *J. Rock Mech. Geotech. Eng*.**, 15**(3), 773-788. https://doi.org/10.1016/j.jrmge.2022.04.012.
Rogers, C.D.F., Dijkstra, T.A. and Smalley, I.J. (1994), "Hydroconsolidation and subsidence of loess: studies from China, Russia, North America and Europe", *Eng. Geol*., **37**(2), 83-113. https://doi.org/10.1016/0013-7952(94)90045-0.
Rogers, C.D.F. (1995), Types and distribution of collapsible soils. In: Genesis of properties of collapsible soils. NATO ASI seriesvol. 468. Dordrecht, the Netherlands: Kluwer Academic Publishers, 1e17.
Ryashchenko, T.G., Akulova, V.V. and Erbaeva, M.A. (2008), "Loessial soils of Priangaria, Transbaikalia, Mongolia and northwestern China", *Quaternary Int*., **179**(1), 90-95. https://doi.org/10.1016/j.quaint.2007.06.035.
Sert, S., Arslan, E., Ocakbaşı, P., Ekinci, E., Garip, Z., Özocak, A., Bol, E. and Ndepete, C.P. (2024), "Stabilization of expansive clays with basalt fibers and prediction of strength by machine learning", *Arab. J. Sci. Eng*., **49**, 13651-13670. https://doi.org/10.1007/s13369-024-08752-w.
Shen, S.L., Han, J. and Du, Y.J. (2008), "Deep mixing induced property changes in surrounding sensitive marine clays", *J. Geotech. Geoenviron. Eng.*, **134**(6), 845-854. https://doi.org/10.1061/(ASCE)1090-0241(2008)134:6(845).
Shen, S.L., Miura, N. and Koga, H. (2003), "Interaction mechanism between deep mixing column and surrounding clay during installation", *Can. Geotech. J*., **40**(2), 293-307. https://doi.org/10.1139/t02-109.
Stipho, A. (1985), "On the engineering properties of salina soil", *Q. J. Eng. Geol. Hydrogeol.* **18**(2), 129-137. https://doi.org/10.1144/GSL.QJEG.1985.018.02.02.

Verma, G., Kumar, B., Kumar, C., Ray, A. and Khandelwal, M. (2023), "Application of KRR, K-NN and GPR algorithms for predicting the soaked CBR of fine-grained plastic soils", *Arab. J. Sci. Eng*., **48**, 13901-13927. https://doi.org/10.1007/s13369-023-07962-y.

CC